

NGU Report 2014.053

Geochemical data from Hattfjelldal

Report no.: 2014.053	ISSN 0800-3416	Grading: Open
Title: Geochemical data from Hattfjelldal		
Authors: Ola Anfin Eggen and Tor Erik Finne		Client: NGU MINN
County: Nordland		Commune: Hattfjelldal, Grane, Hemnes
Map-sheet name (M=1:250.000)		Map-sheet no. and -name (M=1:50.000) 1925-1, 1925-4, 1926-1, 1926-2, 1926-3, 2025-4, 2026-3, 2026-4
Deposit name and grid-reference:		Number of pages: 77 Price (NOK): 310,- Map enclosures:
Fieldwork carried out: 06.-28.8.2013	Date of report: 28.11.2014	Project no.: 338500 Person responsible: <i>Beinda Tilm</i>
Summary: During field work in the summer of 2013, mineral soil samples were collected in a grid of 1x2 km in the municipality of Hattfjelldal in Nordland county, as well as smaller areas in the adjacent municipalities Grane and Hemnes. Together with samples for quality control, the <2mm fraction of samples from 954 locations were digested by aqua regia and analyzed for 53 elements.		
Results are documented with respect to quality of data in tables of descriptive statistics, as well as plots of the cumulative probability function and by single element maps on a backdrop of bedrock geology.		
A selection of anomalies are briefly described, both areas of no known mineralizations, as well as anomalies of new elements in established ore-districts are covered.		

Keywords: geochemistry	mineral soil	MINN
Hattfjelldal	Grane	Hemnes

CONTENTS

1.	INTRODUCTION.....	4
2.	DESCRIPTION OF SURVEY AREA.....	4
3.	METHODS.....	7
3.1	Planning stage and field work	7
3.2	Sample preparation	8
3.3	Chemical analyses	9
3.4	Quality control.....	9
3.4.1	Accuracy.....	10
3.4.2	Precision	10
3.5	Data analysis.....	11
4.	RESULTS AND COMMENTS	11
4.1	Data tables	11
4.2	Cumulative probability (CP-) plot	11
4.3	Maps	12
5.	DISCUSSION - FIRST IMPRESSIONS	13
6.	CONCLUSION	13
7.	ACKNOWLEDGEMENTS	13
8.	REFERENCES	14
	Appendix 1: Cumulative frequency diagrams.....	21
	Appendix 2: Geochemical maps from the Hattfjelldal area.....	29

FIGURES

Figure 1:	Overview and index map. Simplified bedrock geology and records of the NGU mineral resources database: Metal groups.....	5
Figure 2:	Map of all sampling locations and –numbers on top of Quaternary deposits and point observations of ice flow direction..	6
Figure 3:	Photo showing sample, sample pit and all essential tools. Photo O.A. Eggen	8
Figure 4:	Sample preparation sequence, from left to right.....	8
Figure 5:	X-chart for La.....	10
Figure 6:	The EDA symbol set.	12
Figure 7:	Legend of bedrock map used as backdrop of all geochemical maps in Appendix 2.13	13

TABLES

Table 1:	Minimum, median, maximum and precision values for the project standard MINN.	16
Table 2:	Minimum, median (Q50), maximum and precision values for the Acme standards.. ..	17
Table 3:	Precision on analytical and field duplicates.....	18
Table 4:	Statistical parameters for the mapped data.....	19
Table 5:	Comparable geochemical statistics for three MINN surveys. Units in mg/kg.....	20

1. INTRODUCTION

At the end of 2010, NGU was granted additional funding for a new mineral prospecting initiative, organized under the project MINN. Nearly 1000 samples of soil collected in 1980-84 from Finnmark county, and almost 1200 from Troms and Nordland counties were reanalysed (Reimann et.al, 2011). Based on the results from these low sampling density data (c. 1 sample/40km²), NGU's geochemistry team conducted follow-up geochemical mapping in Nordkinn, Finnmark (Reimann et.al, 2012) and Nord-Salten, Nordland (Finne and Eggen, 2012). These campaigns were based on sampling densities 1/2km² and 1/4km², respectively, and the elements of interest were REE, Cu and Au. During late summer 2013, field work was carried out in Hattfjelldal, Nordland county, an area due south of the closed Pb-Zn sulphide mine Bleikvassli, extending eastwards to the Swedish border, and Børgefjell National Park to the south. Applying a 1 sample/2km² density, the aim was to match the westerly extension of a similar regional soil geochemical mapping around Bleikvassli (Krog, 1996). Target commodities for the present survey were base metals and noble metals.

2. DESCRIPTION OF SURVEY AREA

This report covers around 1900 km², namely large parts of Hattfjelldal municipality in Nordland county, but also smaller areas in the adjacent municipalities Grane and Hemnes. An overview map of the area is given in Figure 1, where records of the NGU ore database (anything from showings to large mines) is plotted on a bedrock map. About half of the area is above the treeline at about 800 masl, and only a small part of the area is more than two hours walking distance from nearest road.

The mapsheet "Hattfjelldal" is one of the few published bedrock mapsheets of scale 1:50 000 in the area. It covers the central part of the surveyed area, and also a good part of the variation throughout the entire area. Dallmann and Stølen (1994) state in their description to the bedrock mapsheet Hattfjelldal: "The Hattfjelldal map area is situated within the Caledonian orogen. It includes several thrust nappes from the Lower Kø1i level in the east to the Helgeland Nappe Complex in the west. The Kø1i Nappes consist mostly of low grade metamorphic, Ordovician to (?) Silurian rocks. They are mainly phyllites and carbonate rocks, with subordinate conglomerates, quartzites and greenschists. Carbonate rocks occur particularly within the Hattfjelldal Nappe, where they constitute the Røssvatnet Group..... They are considered as the source strata of a locally thick conglomerate sequence at the base of the overlying Limingen Group. The lenticular Krutfjellet Nappe occupies a special position within the Kø1i nappe pile. It consists of higher grade metamorphic gneisses and amphiboles which envelop an Early or Middle Ordovician gabbro intrusion. The Helgeland Nappe Complex is divided into three units: a lower intrusive complex (Skinnfjellet Unit) of mainly quartz diorite and metagabbro, a banded gneiss complex (Geittinden Unit), and a marble/mica gneiss complex (Appfjellet Unit). The boundaries between these units are tectonic, but it is possible that the two latter represent an original basement-cover relationship. The higher grade metamorphic nappes provide evidence of early Caledonian or older deformation and metamorphism. Some of the metasediments within the low-grade metamorphic nappes, however, seem to be younger than these events. The entire rock sequence was eventually subjected to fold-and-thrust tectonics at low-grade metamorphic conditions during the Scandian orogenic event (Mid Silurian to Devonian)".

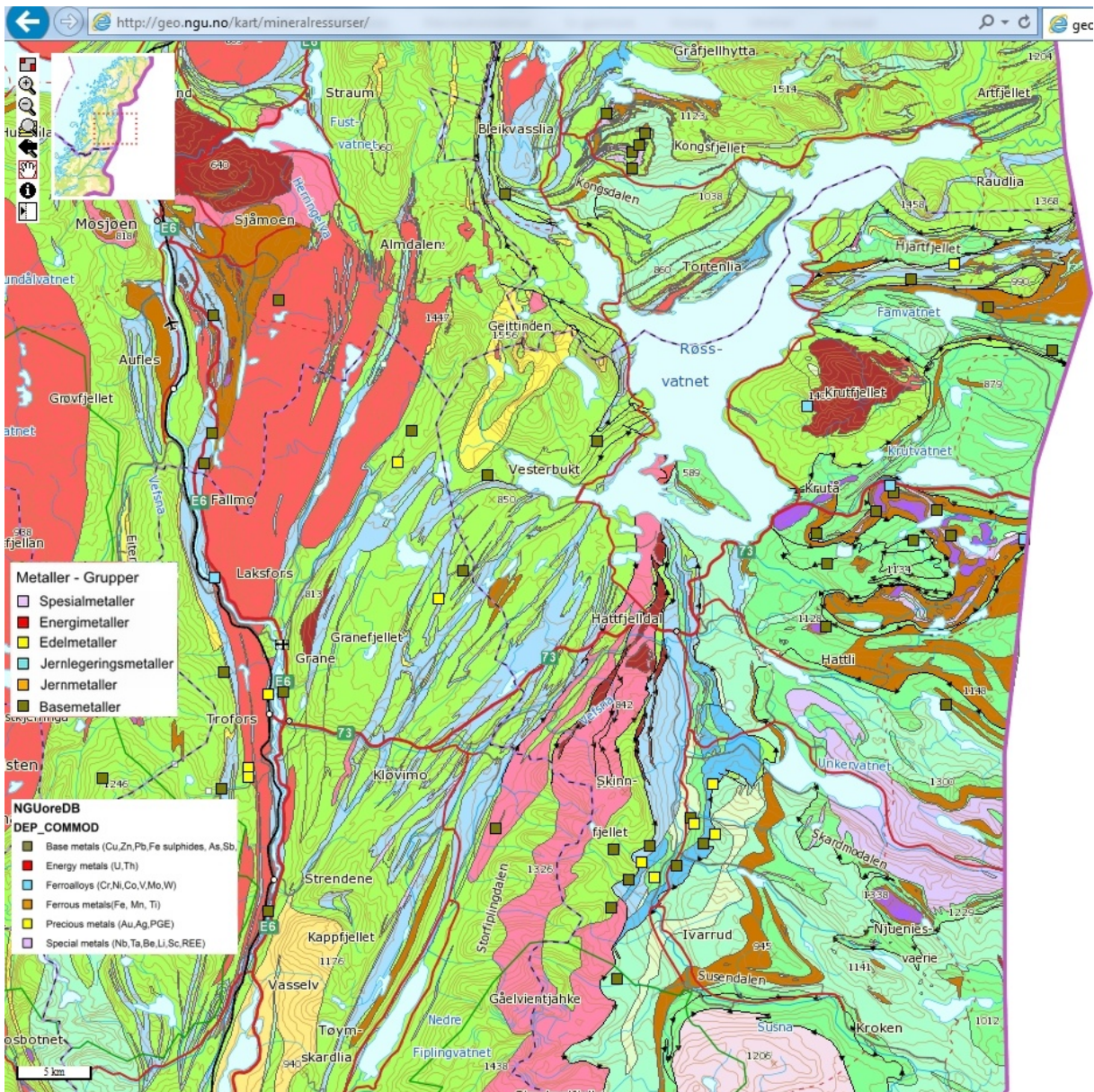


Figure 1: Overview and index map. Simplified bedrock geology and records of the NGU mineral resources database: Metal groups.

The quaternary deposits of the area are generally fairly thick till deposits in the lowland, but rather scarce and nearly absent at higher altitudes. Ice flow direction in the area was towards NW, and towards N during the latest stages, mostly in the lowland (Bargel et.al. 1999). Transport distances are uncertain according to Olsen (in Krog, 1996). Figure 2 shows the quaternary deposit map with some 60 point observations of ice flow indications, as well as location and number of all samples of this survey. In addition, the records of the ore database are plotted.

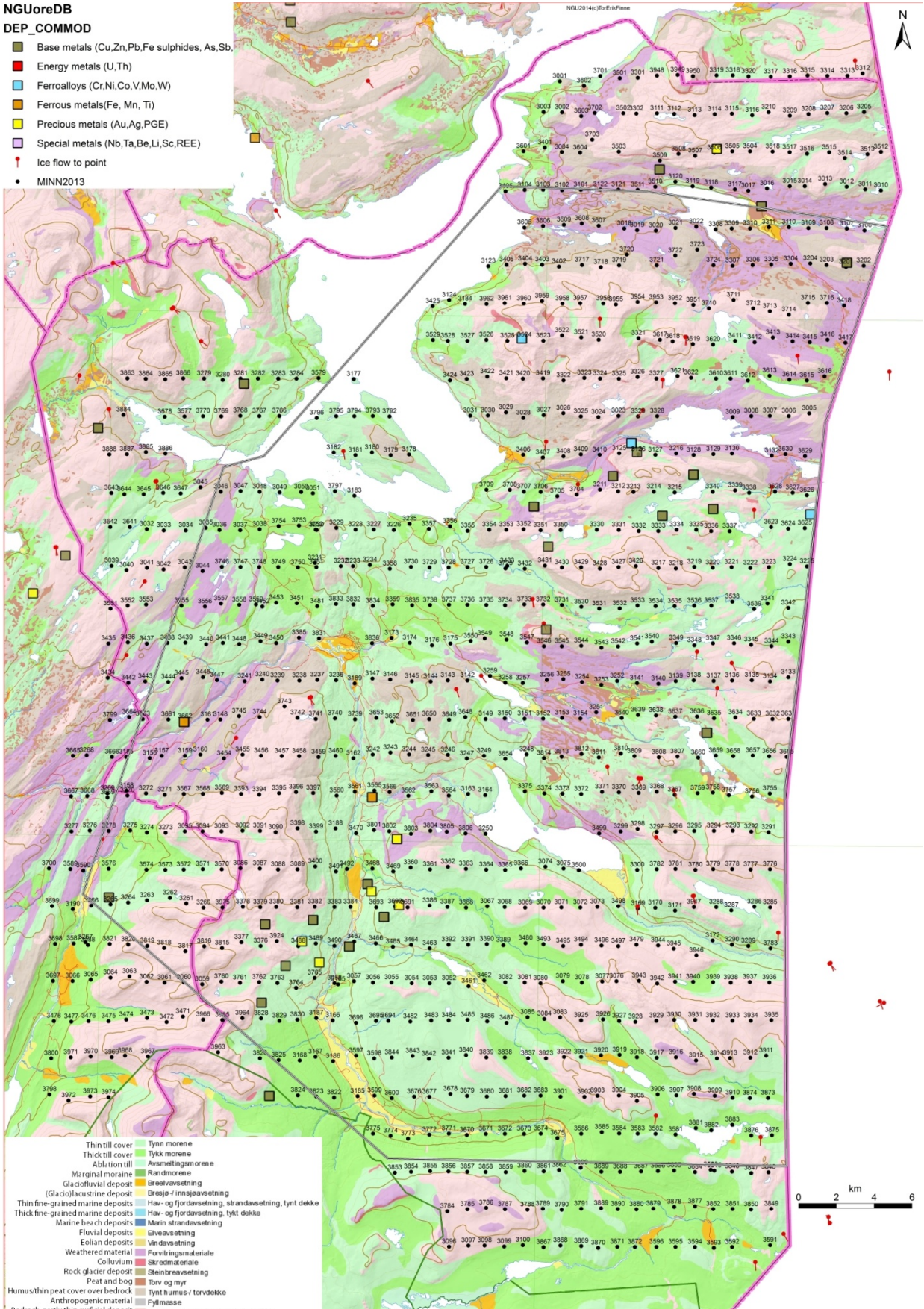


Figure 2: Map of all sampling locations and –numbers on top of Quaternary deposits and point observations of ice flow direction. Grey outline shows extent of recently published helicopter-borne geophysical data (Rodionov et.al., 2014).

Numerous isolated locations have over the years been subjected to prospecting, applying most of the tools of the trade, even core drilling. The elements targeted are usually Au and Ag, and Pb and Zn. The mineralization at Mikkeljord in Susendalen is an example of the latter, where a small ore grade deposit is well documented (Færden, 1953, Cramer et.al 1976, and Staw 1977), but abandoned.

3. METHODS

3.1 Planning stage and field work

A 1x2 km grid was considered a feasible compromise between the size of the area of interest and available resources for the project, and a sampling density adding new information relative to that of the data of the 1/40 km²- survey. This is also a sampling density similar to the surveys of the two previous MINN surveys, a grid of 1x2 km was generated to assist in planning of field logistics. The grid was overlain on topographical maps along polygons delineating glaciofluvial deposits to be excluded from sampling. Within each of the grid squares, field workers were free to find a suitable location, preferably as close as possible to the grid center and with a minimum distance of 10-100 m from abandoned to high traffic roads. Sample pits were dug by paint-free steel spade down well into the mineral soil layer, preferably to C-horizon in podzols. Samples were collected into Rilsan® plastic bags using a small steel trowel. Figure 3 shows a typical sample pit, the equipment used and a typical sample. Sample wet weight was on average 1.6 kg. Sample contamination was minimized by the field crew not wearing any jewellery during sampling, and tools were wiped clean before collecting the next sample. For about every 20th sample a duplicate sample was collected 1-10m from original sample site, resulting in a total of 49 duplicate pairs.

In total 954 localities were sampled. The samplers worked individually. On average, a sampler was able to collect 6-7-samples per day without helicopter support. The daily sample rate increased nearly ten-fold when helicopter was used for the most remote locations, but at the same time cost per sample almost doubled. All in all, the average daily sampling rate was 43. Field work was carried out in the period 6.8 – 28.08.2013, with the crew fluctuating between 3 and 9 people.



Figure 3: Photo showing sample, sample pit and all essential tools. Photo O.A. Eggen

3.2 Sample preparation

Upon arrival at the NGU laboratories, samples were dried in their original sampling bag for three weeks at temperatures below 40 °C. Sample dry weight was on average 1.3 kg. Subsequently all samples were dry sieved to <2mm (9 mesh), from which 2 aliquots of 90+ g were obtained. Surplus <2mm material as well as the >2mm fraction were saved for possible later usage. From all field duplicates, an additional split was generated. Figure 4 shows the sample preparation sequence.

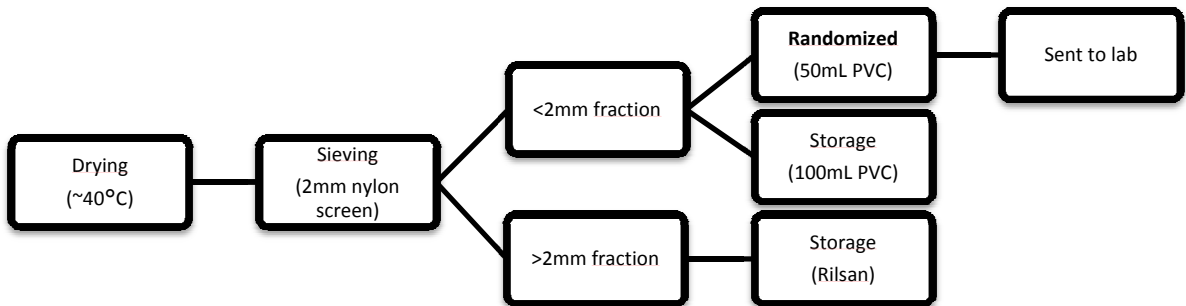


Figure 4: Sample preparation sequence, from left to right.

Nylon sieves were used, and no jewelry was worn during preparation work. Cross contamination via sample dust during sieving was controlled by sieving samples one at a time in a vented box. All sieving equipment was cleaned using a vacuum cleaner in between every sample. Following sample preparation, one single series of all samples were randomized in a structured manner, so that for

about every 17th sample sent to the laboratory, a field duplicate, its split and its ordinary sample as well as a split of the project standard MINN was inserted. The control samples were not always inserted in the exact same positions within the group.

3.3 Chemical analyses

The randomized series of 90+ g aliquots were shipped to ACME laboratories in Vancouver, Canada. The laboratory introduced a further 34 splits of its own quality control (QC) samples DS10 and OSX109 for overall QC. The laboratory also did replicate weighing, extraction and analyses of 33 replicates of ordinary samples throughout the analytical sequence.

The MINN campaigns of 2011 and 2012 (Reimann et al., 2012; Finne and Eggen, 2013) as well as the reanalysis on the Nordland/Troms samples (Reimann et al., 2011) followed the same procedure with successful quality assessment at the named laboratory. For all these campaigns, a 15 g sample weight was used for extraction.

The samples were digested in 90 ml aqua regia and leached for one hour in a hot (95 °C) water bath. After cooling, the solution was made up to a final volume of 300 ml with 5% HCl. The ratio of sample weight to solution volume is 1g per 20 ml. The solutions were analyzed using a Spectro Ciros Vision emission spectrometer (ICP-AES) and a Perkin Elmer Elan 6000/9000 inductively coupled plasma mass spectrometer (ICP-MS). Analytical results were returned from the laboratory within one month after receiving the samples. The remainder of the sample material was stored in the event of mishaps with the first weighing, and for possible upcoming analyses following alternative procedures. Unused sample material was not returned, but destructed by the laboratory after the holding period, according to local regulations.

3.4 Quality control

To be able to estimate analytical precision based on analytical duplicates and to calculate the practical detection limits, it was agreed with the laboratory that all instrument readings were reported, independent of quantification and detection limits. For statistical calculations on the quality control part the instrument readings were used. Negative readings were replaced by a very low positive value prior certain statistical analyses.

X-charts are a simple yet powerful way of studying the quality of the data. The data for a variable is plotted against its analytical sequence number, and by also plotting the median and deviation from the median it is possible to a) identify time trends or breaks in the analysis sequence, b) get an impression of precision by looking at the spread from the median, and c) get an impression of accuracy if the "true", certified value is known. X-charts from this survey (for an example see Figure 5, plot to the right) indicate that no severe problems are present with regards to time trends or breaks in analytical results. All in all, most results for the standards were satisfactory. Table 1 and Table 2 identify the problematic elements.

3.4.1 Accuracy

The project standard MINN was used to estimate the accuracy of the analysis and to detect possible time trends or breaks in the analysis sequence. This standard material was also used in the Nordkinn (Reimann et al., 2012) and Nord-Salten (Finne & Eggen, 2013) surveys and therefore gives the opportunity to compare the three surveys. The laboratory also used its own house standards, DS10 and OXC109, inserted throughout the analysis series. Table 1 and Table 2 display values for minimum, median and maximum, as well as precision for the analytical results for the standards MINN, DS10 and OXC109. For comparison with prior analytical results of the MINN standard, the median values from the Nordkinn study (Reimann et al., 2012) are also given in Table 1. As an illustration of similarity in the MINN standard behavior, Figure 5 shows X-charts of La for Nordkinn, Nord-Salten and this survey, respectively. In the MINN standard Au, B, Cd, Pd, Pr, Re, Ta are present at very low concentrations which bring along very low precision. In laboratory standard DS10 only Ta and Ge has so low concentrations that it remains problematic (Table 2), while for laboratory standard OXC109 this applies to Re, Te, Se, Hg, Pt, and Pd.

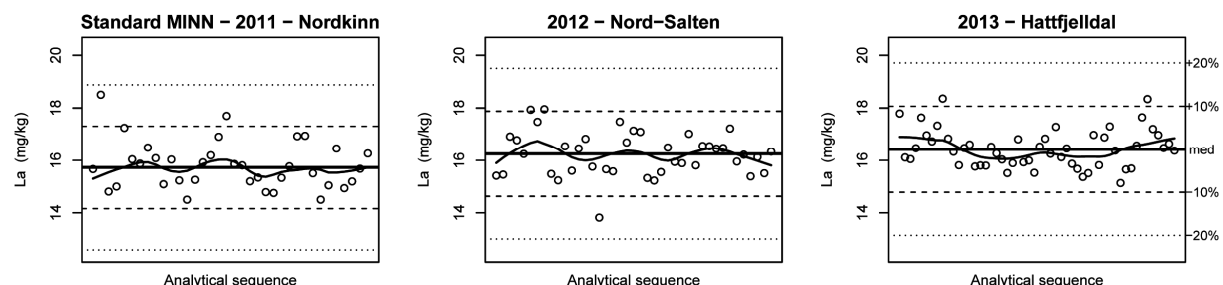


Figure 5: X-chart for La depicting stability for project standard "MINN" in year 2011 Nordkinn, year 2012 Nord-Salten and this study, showing similarity in median and precision in the three datasets. Dashed and dotted lines marks $\pm 10\%$ and $\pm 20\%$ deviation, respectively

3.4.2 Precision

Table 3 shows the estimate of precision based on the analytical duplicates and the field duplicates. The low precision is principally due to the natural variability shown in the difference between ordinary field sample and field duplicate samples. In most cases the observed problems with precision were due to very low concentrations as in the case of our project standard MINN, i.e. analytical results at or below the limit of quantification, like Au, B, Ge, Pd, Pt, Re, Se, Ta and Te. However, the field duplicate results reveal that some elements are plagued by poor reproducibility, and maps should be viewed with care. These are included in the listing below.

Practical detection limit (PDL) was established based on method described by Demetriades (2011), using the results for analytical replicates. Good results of the duplicates led us to use a lower PDL rather than the laboratory's method detection limit (MDL) for Al, Ca, K, Na, S and Zr. On the other hand, PDL had to be increased for a range of elements; Ag, Au, B, Cd, Co, Hf, Hg, Mn, Nb, Ni, Pb, Pt, Rb, Re, Se and Te.

3.5 Data analysis

Geochemical data are compositional data, meaning that they do not contain truly independent values but only relative information; the reported concentrations of all elements analyzed depend on one another (Aitchison, 1986; Filzmoser et al., 2009). Such data have some special properties which can lead to wrong results when applying the methods developed for classical statistical data analysis (Reimann et al., 2013). Thus EDA (exploratory data analysis) techniques and simple order statistics as suggested by Reimann et al. (2008) are used here. All statistical calculations are determined by use of the freely available R software (R development core team, 2014) and the additional StatDA package (Filzmoser, 2013).

4. RESULTS AND COMMENTS

4.1 Data tables

A statistical overview for the dataset is provided in Table 4. The table is built around the minimum, maximum and median value, and also provides the values for a number of additional quantiles (percentiles) for the analyzed elements. As an additional measure of variation the “powers” are provided, which provide a direct impression of the orders of magnitude variation for each variable. When using classical statistical methods for calculation of the mean and standard deviation to derive at “thresholds” for anomalies, 2.6% of all data is often identified as anomalies at both ends of the distribution if the dataset has a normal distribution. The data at hand are far from normally distributed and therefore unsuited for classical statistics – thus the quantiles Q2 and Q98 (or Q5 and Q95) can be taken as lower and upper threshold for the data. However, quite often Cumulative Probability (CP) plots (see below) provide a better means of identifying anomalies in the data by inspection of shape of the curve.

Table 5 displays the analytical results with a more common approach, showing median, 98th percentile value and maximum concentration for the Hattfjelldal dataset and data for directly comparable Nord-Salten (Finne and Eggen, 2013) and Nordkinn datasets (Reimann et. al, 2012). They are comparable in terms of grain size, laboratory procedures, and number of samples. For median, Q98 and maximum, the highest value for each element between the three datasets is underlined.

4.2 Cumulative probability (CP-) plot

Plots of the cumulative distribution function are one of the most informative displays of geochemical distributions (Reimann et al., 2008). In the plots the concentration is plotted along the X-axis and the cumulative probability is plotted along the Y-axis, and it allows the direct visual recognition of breaks in the curve which may be indicative of different geochemical processes. Breaks in the uppermost few percentiles of the distribution are often used as thresholds for anomaly identification. Readings below the PDL are here set to half the PDL value for that element, respectively. Appendix 1 provides the CP-plots for all 53 variables.

4.3 Maps

Many different methods for producing geochemical maps exist (see discussion in Reimann, 2005 or in Chapter 5 of Reimann et al., 2008). In mineral exploration so called "growing dot maps" as introduced by Bjørklund and Gustavsson (1987) are probably most often used. However, they focus the attention almost exclusively on the high values, the "anomalies" and are less well suited to study the data in more detail, e.g., in relation to geology. It may also be argued that the "growing dot map" has limitations in detecting local anomalies as they often do not display especially high values in relation to the whole dataset, but rather high values in relation to their local surroundings. Some of these shortcomings can be helped by giving special attention to the growth increment of the symbols, and the overall size of the symbols in the map image.

	EDA symbol set	EDA symbol set extremes are accentuated	EDA symbol set extremes are accentuated Used in this report	Precentiles used in this report
Highest values	+	■	■	95–100%
Higher values	+	+	■	75–95%
Inner values	.	.	.	25–75%
Lower values	○	○	○	5–25%
Lowest values	○	○	○	0–5%

Figure 6: The EDA symbol set.

The EDA symbol set aim to provide an optical weight for each symbol in the map (Reimann et. al, 2008). Lower values are shown by circles, the inner (most common and in many cases the "least interesting") values are shown as dots, while the higher values are shown by crosses in the original EDA symbol set. Figure 6 shows the original EDA symbols to the left, and modifications in the middle. The percentiles used for the classes are 5 – 25 – 75 – 95% for all maps in this report. All maps are prepared on a backdrop of a generalized bedrock map based on the available maps in scale 1:250 000 hosted by <http://geo.ngu.no/kart/berggrunn/>. An excerpt of the legend for the 1:250 000 scale map series is shown in Figure 7. All maps are given in Appendix 2. Please note that elements B, Pd, Pt, Re and Ta are kept out of the map collection due to very poor analytical data quality.

The dataset for this report is provided online

<http://www.ngu.no/en-gb/tm/Prosjekter2/Mineralressurser-i-Nord-Norge-MINN/> (Look for "Last ned data her"), and it is therefore possible and up to the reader to use different mapping techniques. Note, however, that in the provided data file all values below detection are marked as "<n", n being the PDL, while NGU had the original instrument readings available, i.e. values for every sample. NGU used the instrument reading values as these results often contain valuable information when using large datasets with hundreds of samples. For example, the laboratory's official detection limit for S is 200 mg/kg, but the QC results indicate that values down to 20 mg/kg are still reliable. Thus

a full order of magnitude real, natural variation would have been lost when setting all values below the MDL to for instance $\frac{1}{2}$ of the detection limit.

Berggrunn tegnforklaring

 3 - Konglomerat, sedimentær breksje
 26 - Ryolitt, ryodacitt, dacitt
 35 - Gabbro, amfibolitt
 38 - Kvartsdioritt, tonalitt, trondhjemitt
 40 - Olivinstein
 55 - Grønnstein, amfibolitt
 62 - Glimmergneis, glimmerskifer, metasandstein, amfibolitt
 65 - Fyllitt, glimmerskifer
 66 - Kalkglimmerskifer, kalksilikatgneiss
 70 - Marmor
 71 - Dolomitt

Bedrock Legend

 3 - Conglomerate, sedimentary breccia
 26 - Ryolite, ryodacite, dacite, keratophyre
 35 - Gabbro, amfibolite
 38 - Quartz diorite, tonalite, trondhjemite
 40 - Peridotite, pyroxenite
 55 - Greenstone, amphibolite
 62 - Mica gneiss, mica schist, metasandstone, amfibolite
 65 - Phyllite, mica schist
 66 - Calcareous mica schist, calc silicate gneiss
 70 - Marble
 71 - Dolomite marble

Figure 7: Legend of bedrock map used as backdrop of all geochemical maps in Appendix 2.

5. DISCUSSION - FIRST IMPRESSIONS

A comprehensive discussion of the results is not the aim of this report, however, a few notes are necessary. First of all, all samples were taken from material that are considered to be of fairly local origin, as all fluvial and glaciofluvial deposits were avoided, based on existing quaternary deposit map and observations in the field. Based on good correlation between soil chemistry and the bedrock map, indications are strong that material also outside the areas where the soil consists of in situ weathered rock are transported only short distances.

The most prominent feature in the map collection is the multielement anomaly in Hattli, that carries no Cr, Ni, Pb or S, but is high in Zn and a score of other elements. The W map, although no really high values, makes up a pattern that either oppose the notion that there are short transport distances in the till, or that the fingerprint of the intrusion are seen also in the surrounding sedimentary rocks.

6. CONCLUSION

The data presented here are well suited to for a combined interpretation with the geophysical data recently presented by Rodionov et.al (2014) to aid in planning upcoming ore geology mapping

7. ACKNOWLEDGEMENTS

We greatly appreciate the cooperative spirit of the local authorities and population; without it we could have risked the onset of snow before the field work was completed. We thank our hosts at Sæterstad gård and Gryteselv fjellgård not only for excellent food & beds but also for arranging room for field office and temporal sample storage. Thanks to the people at Sivertsgården for lending us boat on Famvatnet, and Hattfjelldal jakt- og fiskelag for lending us boat on Øverelsvatnet. The field crew did a formidable job: Malin Andersson, Atle Dagestad, Belinda Flem, Guri Venvik Ganerød, Henning K. B. Jensen, Åse Minde, Magnus Nicolaisen, Iselin Esp Pettersen, Gaute Storrø, Hild Sissel Thorsnes, and Ola Vikhammer, as well as the authors. Jostein Jæger and Iselin worked relentlessly at the sample preparation lab by sieving, splitting and weighing the samples.

8. REFERENCES

- Aitchinson, 1986. The statistical analysis of compositional data. Chapman and Hall, London.
- Bargel, T., Huhta, P., Johansson, P., Lagerbäck, R., Mäkinen, K., Nenonen, K., Olsen, L., Rokoengen, K., Svedlund, J.-O., Väänänen, T. & Wahlroos, J.-E., 1999: *Maps of Quaternary geology in Central Fennoscandia, sheet 3: Ice-flow Indicators, scale 1:1 000 000, and Quaternary stratigraphy, scale 1:2 000 000*. Geological Surveys of Finland (Espoo), Norway (Trondheim) and Sweden (Uppsala).
- Bjørklund and Gustavsson, 1987. *Visualization of geochemical data on maps: new options*. J. of Geochem. Exploration, vol 29, pp. 89-103
- Cramer, J., Vik, E, Staw, J. 1976. *Råstoffundersøkelser i Nord-Norge. Mineralundersøkelser i Mikkeljord, Hattfjelldal kommune*. (in Norwegian). NGU rapport 1339/1. 10pp.
- Demetriades, A., 2011. *Understanding the Quality of Chemical Data from the urban environment - Part 2: Measurement Uncertainty in the Decision-making Process*. In *Mapping the Chemical Environment of Urban Areas*. Johnson, C.C., Demetriades, A., Locutura, J. and Ottesen, R.T. (Eds.). Wiley-Blackwell, Oxford, united Kingdom. ISBN 978-0-470-74724-7
- Dallmann, W.K. 1994. *Hattfjelldal. Berggrunnskart; Hattfjelldal; 19262; 1:50 000; trykt i farger*.Map. NGU.
- Dallmann, W.K. and Stølen, L.K. 1994. *Hattfjelldal - berggrunnsgeologisk kart 1926 II - M 1:50 000. Beskrivelse*. (In Norwegian with English summary). NGU report 93.044. 47 pp.
- Filzmoser P., Hron, K., Reimann, C., 2009. *Univariate statistical analysis of environmental (compositional) data – Problems and possibilities*. Science of the Total Environment 407, 6100-6108.
- Filzmoser, 2013. StatDA: Statistical Analysis for Environmental Data. R package version 1.6.7, <http://CRAN.R-project.org/package/StatDA>
- Finne, T.E. and Eggen, O.A. 2013. *Soil geochemical data from Nord-Salten, Nordland*. NGU Report 2013.015. 101 pp.
- Færden, J. 1953. *Sink-blyforekomstene ved Mikkeljord, Hattfjelldal i Nordland*. . (In Norwegian with English summary). NGU Årbok 1952,NGU Bulletin 184, pp. 145-153.
- Kjeldsen, S. 1987. *Geokjemisk kartlegging i Nordland og Troms. ICAP-analyse av løsmassenes finfraksjon*. (in Norwegian). NGU rapport 87.142. 69 pp.
- Kjeldsen, S. and Ottesen, R.T., 1988. *Geokjemisk kartlegging i Nordland og Troms. Data for innholdet av gull i løsmassenes finfraksjon*. (in Norwegian). NGU Report 88.084. 17 pp.
- Krog, R. 1996. *Soil geochemistry of the Bleikvassli area (Status Report No.1) Regional investigations of the area between Røssvatnet and Målvatnet*. NGU report 95.155. 85 pp.
- R Core Team, 2014. R: A Language and Environment for Statistical Computing, R Foundation for Statistical Computing, Vienna, Austria, <http://www.R-project.org/>

Reimann, C., Filzmoser, P., Garrett, R.G., Dutter, R., 2008. Statistical data analysis explained. Applied environmental statistics with R. Wiley, Chichester, U.K.

Reimann, C., Finne, T.E., Filzmoser, P., 2011. *New geochemical data from a collection of till samples from Nordland, Troms and Finnmark*. NGU report 2011.45. 152 pp.

Reimann, C., Finne, T.E., Filzmoser, P., 2012. *Soil geochemical data from the Nordkinn peninsula, Finnmark*. NGU Report 2012.016.

Reimann, C., Birke, M., Demetriades, A., Filzmoser, P. & O'Connor, P. (eds.) (2013): Chemistry of Europe's Agricultural Soils. Part A: Methodology and interpretation of the GEMAS Data Set.-Geol. Jb., **B 102**,: 528 pp: 358 figs., 86 Tables, 1 DVD; Hannover

Rodionov, Alexei; Ofstad, Frode; Stampolidis, Alexandros; Tassis, Georgios. (2014). *Helicopter-borne magnetic, electromagnetic and radiometric geophysical survey in Hattfjelldal, Nordland County*. NGU report 2014.029. 29 pp.

Staw, J. 1977. *Undersøkelse av Statens bergrettigheter. Geokjemiske undersøkelser, Mikkeljord, Hattfjelldal kommune, Nordland*. (in Norwegian). NGU-rapport 1430/19A. 5pp

Table 1: Minimum, median, maximum and precision values for the project standard MINN. Concentrations in mg/kg.

MINN standard (n=53) alphabetical								Sorted by precision			
Element			Precision	Nordkinn	Element			Precision	Nordkinn	Element	Element
Min	Q50	Max		Q50	Min	Q50	Max		Q50	Precision	Precision
Ag	<0.005	0.010	0.017	37	0.005	Na	16	54	63	11.1	35
Al	16610	17450	18060	2.5	17085	Nb	1.3	1.8	2.3	13	1.8
As	1.3	2.0	2.5	10	2.2	Ni	18.0	20.1	22.7	4.6	19
Au	<0.002	<0.002	0.003	231	<0.0002	P	339	373	428	5.5	368
B	<7	<7	<7	136	<1	Pb	12.1	13.3	14.8	4.9	13
Ba	46.3	51.2	56.8	5.3	49	Pd	<0.010	<0.010	0.015	861	<0.01
Be	<0.10	0.35	0.66	25	0.33	Pt	<0.004	<0.004	<0.004	1339	<0.002
Bi	0.06	0.08	0.12	15	0.09	Rb	62.9	71.9	79.0	4.5	67
Ca	522	788	1105	7.4	744	Re	<0.01	<0.01	<0.01	-884	<0.001
Cd	<0.05	0.007	0.040	160	0.01	S	62.8	87.6	142	2.0	100
Ce	25.8	27.9	30.7	4.8	26	Sb	<0.02	0.02	0.04	32	0.03
Co	11.6	12.8	14.8	5.5	12	Sc	2.3	2.7	3.2	7.0	2.1
Cr	21.3	23.1	27.4	3.5	23	Se	<0.5	<0.5	0.5	86	0.3
Cs	4.1	4.5	4.9	4.3	4.2	Sn	0.4	0.6	0.8	16	0.6
Cu	10.5	12.1	13.1	5.4	11	Sr	3.1	3.5	4.0	4.3	3.6
Fe	29991	31418	33120	1.6	30902	Ta	<0.05	<0.05	<0.05	222	<0.05
Ga	5.24	5.74	6.24	4.3	5.5	Te	<0.07	<0.07	<0.07	-708	0.01
Ge	<0.10	0.17	0.34	43	0.08	Th	4.0	4.4	5.6	4.3	3.8
Hf	0.07	0.13	0.21	18	0.09	Ti	2012	2253	2571	5.0	2163
Hg	<0.01	<0.01	0.03	94	<0.005	Tl	0.47	0.53	0.58	4.4	0.53
In	<0.02	<0.02	0.03	43	<0.02	U	2.35	2.63	3.04	5.0	2.5
K	5410	5721	5892	2.2	5544	V	32.5	33.9	35.1	2.4	33
La	15.1	16.5	18.4	4.6	16	W	<0.05	<0.05	0.07	31	<0.1
Li	14.1	15.8	17.5	4.3	16	Y	7.9	8.7	9.5	4.0	8.4
Mg	5680	6031	6323	2.5	5946	Zn	55.7	64.7	75.1	5.7	59
Mn	219	238	260	4.2	235	Zr	4.8	6.2	8.1	14	4.1
Mo	1.63	1.89	2.22	3.7	1.8						P
											5.5

Table 2: Minimum, median (Q50), maximum and precision values for the Acme standards DS10 and OXC109. Concentrations in mg/kg

DS 10 standard (n=34)								OXC 109 standard (n=34)										
Alphabetical				Sorted by precision				Alphabetical				Sorted by precision						
Element	Precision	Element	Precision	Element	Precision	Element	Precision	Element	Precision	Element	Precision	Element	Precision	Element	Precision			
Min	Q50	Max		Min	Q50	Max		Min	Q50	Max		Min	Q50	Max				
Ag	1.94	2.01	2.33	3.8	Na	580	633	776	4.8	Ta	137	Sc	5.1	Ag	0.013	0.020	0.033	15
Al	9970	10392	11138	2.4	Nb	1.4	1.6	1.9	11	Ge	47	Ti	5.1	Al	13006	14220	15374	4.1
As	41.9	44.6	49.0	4.1	Ni	71.8	76.6	84.6	2.9	Be	21	P	5.0	As	0.2	0.6	1.8	20
Au	0.088	0.104	0.156	12	P	675	758	846	5.0	B	15	Na	4.8	Au	0.184	0.204	0.219	4.3
B	<7	<7	10.3	15	Pb	146	160	171	4.6	Au	12	Pb	4.6	B	<7	<7	<7	49
Ba	344	377	406	4.3	Pd	0.09	0.10	0.14	10	Hf	12	Cd	4.5	Ba	48.2	54.7	61.1	4.0
Be	0.5	0.6	1.3	21	Pt	0.174	0.197	0.217	6.5	Nb	11	Ba	4.3	Be	0.5	0.8	1.4	20
Bi	10.4	12.4	14.3	8.1	Rb	26.3	28.7	31.8	3.9	Th	11	Li	4.1	Bi	<0.02	<0.02	0.08	78
Ca	10553	10839	11183	2.1	Re	0.04	0.06	0.07	9.5	Pd	10	As	4.1	Ca	4956	5527	6229	4.5
Cd	2.27	2.50	2.80	4.5	S	2547	2795	3009	3.8	V	10	Y	4.1	Cd	<0.05	<0.05	0.07	23
Ce	32.1	36.8	40.7	3.9	Sb	4.78	6.21	7.01	5.1	La	10	Rb	3.9	Ce	20.2	22.4	26.2	7.4
Co	12.1	13.2	14.7	5.8	Sc	2.5	2.8	3.4	5.1	Re	9.5	Ce	3.9	Co	17.8	19.5	22.1	6.5
Cr	50	56	63	5.9	Se	1.86	2.35	3.16	8.6	U	9.4	Mo	3.9	Cr	48.5	55.8	63.0	5.1
Cs	2.63	2.76	2.94	2.4	Sn	1.4	1.6	1.8	8.4	In	8.8	S	3.8	Cs	0.15	0.16	0.19	5.5
Cu	151	157	170	2.3	Sr	58	64	75	7.6	Se	8.6	Ag	3.8	Cu	31.7	35.9	38.0	6.9
Fe	26503	27785	29021	3.0	Ta	<0.05	<0.05	<0.05	137	Sn	8.4	Zr	3.8	Fe	25965	28043	30181	2.7
Ga	3.7	4.3	4.6	5.2	Te	3.84	4.91	5.39	5.3	Bi	8.1	Zn	3.4	Ga	4.54	4.98	5.46	5.5
Ge	<0.10	<0.10	0.15	47	Th	6.6	7.9	9.0	11	Sr	7.6	Mn	3.3	Ge	<0.10	<0.10	0.15	49
Hf	0.05	0.08	0.10	12	Ti	678	743	851	5.1	Hg	7.2	Fe	3.0	Hf	0.18	0.30	0.44	12
Hg	0.27	0.31	0.37	7.2	Tl	4.8	5.1	5.6	5.3	Pt	6.5	Ni	2.9	Hg	<0.010	<0.010	0.016	421
In	0.18	0.23	0.30	8.8	U	2.23	2.65	2.94	9.4	Cr	5.9	K	2.6	In	0.0	0.0	0.0	88
K	3294	3421	3732	2.6	V	37	43	48	10	W	5.8	Cs	2.4	K	3980	4252	4492	2.4
La	15.3	17.6	20.9	10	W	2.7	3.0	3.3	5.8	Co	5.8	Al	2.4	La	10	12	14	9.0
Li	16.7	20.1	21.7	4.1	Y	7.4	7.8	8.8	4.1	Tl	5.3	Cu	2.3	Li	1.7	2.2	3.0	5.1
Mg	7670	7926	8197	1.3	Zn	343	375	404	3.4	Te	5.3	Ca	2.1	Mg	13577	14129	15016	1.9
Mn	840	886	981	3.3	Zr	3.1	3.4	4.0	3.8	Ga	5.2	Mg	1.3	Mn	380	414	454	3.8
Mo	15.4	16.6	17.8	3.9	Sb					Sb	5.1			Mo	1.33	1.50	1.67	3.9

Table 3: Precision on analytical and field duplicates.

ANALYTICAL DUPLICATES (49 pairs)				FIELD DUPLICATES (49 pairs)							
Alphabetical		Sorted		Alphabetical		N.Salten	N.kinn	Sorted		N.Salten	N.kinn
Ele.	Prec.	Ele.	Prec.	Ele.	Prec.	34 pairs	30 pairs	Ele.	Prec.	34 pairs	30 pairs
Ag	19	Re	-933	Ag	43	29	42	Re	-543	-163	389
Al	1.6	Pd	456	Al	20	4	12	Pd	249	116	251
As	4.3	Au	307	As	54	11	40	Pt	225	-342	34
Au	307	Pt	193	Au	186	221	82	Au	186	221	82
B	92	Ta	124	B	97	99	54	Te	152	95	99
Ba	4.5	Te	107	Ba	35	4	19	Ta	111	46	69
Be	37	B	92	Be	45	23	32	B	97	99	54
Bi	8.4	Ge	79	Bi	43	20	21	S	92	17	46
Ca	4.6	Be	37	Ca	39	6	34	Ge	77	31	55
Cd	20	Se	35	Cd	75	25	58	Cd	75	25	58
Ce	3.3	W	34	Ce	24	10	29	Se	67	21	32
Co	3.7	In	33	Co	24	8	16	As	54	11	40
Cr	3.1	Hg	31	Cr	23	4	15	Ga	51	5	11
Cs	4.0	Hf	23	Cs	21	4	9	Sn	49	9	13
Cu	3.8	Cd	20	Cu	46	4	22	K	46	4	15
Fe	1.5	Ag	19	Fe	23	4	10	Cu	46	4	22
Ga	3.0	Na	18	Ga	51	5	11	Na	46	8	14
Ge	79	Zr	17	Ge	77	31	55	Be	45	23	32
Hf	23	Sn	12	Hf	40	21	27	Nb	44	7	23
Hg	31	Sb	10	Hg	43	30	48	Hg	43	30	48
In	33	S	10	In	43	28	36	Ag	43	29	42
K	1.8	Bi	8.4	K	46	4	15	Bi	43	20	21
La	2.9	Nb	7.0	La	32	10	34	In	43	28	36
Li	3.6	Tl	6.0	Li	21	6	15	V	42	3	10
Mg	1.8	Mo	5.7	Mg	20	3	16	Hf	40	21	27
Mn	3.6	Th	4.7	Mn	33	8	22	Ti	40	4	11
Mo	5.7	Ca	4.6	Mo	38	9	35	Ca	39	6	34
Na	18	Ba	4.5	Na	46	8	14	Mo	38	9	35
Nb	7.0	Sc	4.5	Nb	44	7	23	Sr	37	158	19
Ni	4.1	As	4.3	Ni	25	5	13	Ba	35	25	19
P	3.5	Rb	4.2	P	23	5	24	Zr	35	9	20
Pb	3.6	Ni	4.1	Pb	34	9	11	Pb	34	9	11
Pd	456	Sr	4.1	Pd	249	116	251	W	34	18	29
Pt	193	Zn	4.1	Pt	225	-342	34	Zn	34	4	12
Rb	4.2	Cs	4.0	Rb	31	5	14	Mn	33	8	22
Re	-933	U	4.0	Re	-543	-163	389	La	32	10	34
S	10	Y	3.9	S	92	17	46	U	32	6	18
Sb	10	Cu	3.8	Sb	29	16	18	Rb	31	5	14
Sc	4.5	Co	3.7	Sc	20	5	11	Sb	29	16	18
Se	35	Li	3.6	Se	67	21	32	Y	27	5	29
Sn	12	Mn	3.6	Sn	49	9	13	Th	26	8	21
Sr	4.1	Pb	3.6	Sr	37	158	19	Ni	25	5	13
Ta	124	P	3.5	Ta	111	46	69	Tl	25	5	15
Te	107	Ce	3.3	Te	152	95	99	Ce	24	10	29
Th	4.7	Ti	3.3	Th	26	8	21	Co	24	8	16
Ti	3.3	Cr	3.1	Ti	40	4	11	Fe	23	4	10
Tl	6.0	Ga	3.0	Tl	25	5	15	P	23	5	24
U	4.0	La	2.9	U	32	6	18	Cr	23	4	15
V	1.9	V	1.9	V	42	3	10	Cs	21	4	9
W	34	K	1.8	W	34	18	29	Li	21	6	15
Y	3.9	Mg	1.8	Y	27	5	29	Mg	20	3	16
Zn	4.1	Al	1.6	Zn	34	4	12	Al	20	4	12
Zr	17	Fe	1.5	Zr	35	9	20	Sc	20	5	11

Table 4: Statistical parameters for the mapped data. Mineral soil <2mm, aqua regia extraction on 15 g sample material. N=954, concentrations in mg/kg.

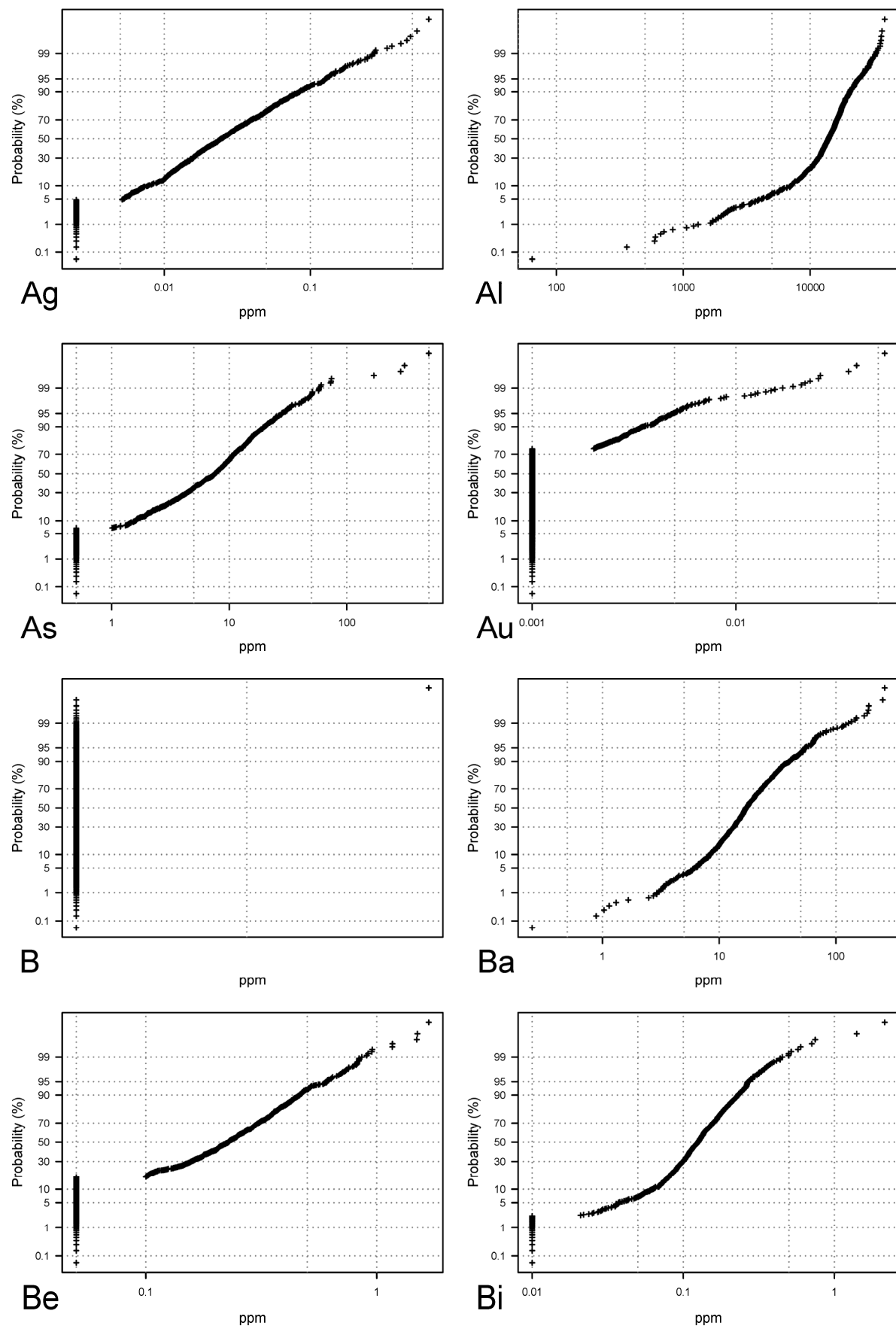
Element	n<PDL	MDL	PDL	Min	Q2	Q5	Q10	Q25	Q50	Q75	Q90	Q95	Q98	Max	Powers	
Ag	46	0.002	0.005	<0.005	0.0025	0.00526	0.00774	0.0137	0.025	0.0471	0.0845	0.127	0.194	0.65	2.4	
Al	0	100	50	64.5	2093	4151	7079	10739	13935	17019	20539	24115	29423	38640	2.8	
As	66	0.1	1	<1	<1	<1	1.6	3.7	7.52	12	20	28	47	498	3.0	
Au	715	0.0002	0.002	<0.002	<0.002	<0.002	<0.002	<0.002	<0.002	0.002	0.003	0.005	0.008	0.054	1.7	
B	953	1	7	<7.0	<7.0	<7.0	<7.0	<7.0	<7.0	<7.0	<7.0	<7.0	<7.0	7.3	0.3	
Ba	1	0.5	0.5	<0.5	3.8	6.2	8.3	12	17	25	40	54	78	262	3.0	
Be	163	0.1	0.1	<0.10	<0.10	<0.10	<0.10	0.14	0.23	0.34	0.46	0.61	0.76	1.7	1.5	
Bi	22	0.02	0.02	<0.02	<0.02	0.04	0.06	0.09	0.13	0.17	0.23	0.27	0.35	2.2	2.3	
Ca	4	100	50	<50	116	256	457	936	1504	2058	2885	3840	6689	313558	4.1	
Cd	546	0.01	0.05	<0.05	<0.05	<0.05	<0.05	<0.05	<0.05	0.07	0.11	0.14	0.22	0.74	1.5	
Ce	0	0.1	0.1	1.1	4.1	7.5	11.6	21.7	37.1	52.0	71.0	88.8	110	225	2.3	
Co	20	0.1	0.4	<0.4	0.2	2.1	3.9	7.2	11	16	21	26	35	69	2.5	
Cr	4	0.5	0.5	<0.5	2.7	5.8	12	23	34	46	59	74	101	885	3.5	
Cs	4	0.02	0.02	<0.2	0.2	0.4	0.5	0.8	1.1	1.6	2.4	2.9	3.8	9.8	3.0	
Cu	1	0.01	0.01	<0.01	0.72	2.45	5.46	12.5	23.4	37.2	52.3	63.8	81.3	210	4.6	
Fe	0	100	100	177	1954	8640	14182	21518	27476	33076	42596	51767	62888	95312	2.7	
Ga	2	0.1	0.1	<0.10	1.17	2.05	2.49	3.18	4.00	4.84	6.51	8.36	11.6	26.4	2.7	
Ge	786	0.1	0.1	<0.10	<0.10	<0.10	<0.10	<0.10	<0.10	<0.10	0.13	0.16	0.18	0.31	0.8	
Hf	214	0.020	0.030	<0.030	<0.030	<0.030	<0.030	0.033	0.053	0.082	0.12	0.15	0.18	0.37	1.4	
Hg	185	0.005	0.010	<0.010	<0.010	<0.010	<0.010	0.011	0.018	0.027	0.039	0.045	0.059	0.23	1.7	
In	629	0.020	0.020	<0.020	<0.020	<0.020	<0.020	<0.020	<0.020	<0.023	0.032	0.038	0.052	0.26	1.4	
K	4	100	25	<25	146	222	302	430	663	1075	1741	2475	3596	10871	2.9	
La	2	0.5	0.5	<0.5	1.8	3.0	4.3	7.9	14	22	28	37	53	128	2.7	
Li	4	0.10	0.10	<0.10	0.86	2.2	4.9	8.8	12	16	19	23	27	73	3.2	
Mg	8	100	100	<100	266	1068	2514	4827	7204	9842	12285	15166	19812	85382	3.2	
Mn	10	1	10	<10	16	57	109	194	335	518	723	941	1344	5042	3.0	
Mo	3	0.01	0.01	<0.01	0.08	0.14	0.21	0.33	0.54	0.90	1.7	2.4	3.6	18	3.6	
Na	91	10	5.0	<5.0	<5.0	<5.0	5.3	19	32	49	74	92	142	626	2.4	
Nb	18	0.02	0.05	<0.05	0.06	0.13	0.21	0.39	0.72	1.2	1.9	2.5	3.7	16	2.8	
Ni	4	0.1	0.3	<0.3	0.9	3.3	7.2	15	25	37	52	62	80	364	3.4	
P	0	10	10	21	67	116	190	337	516	674	831	960	1481	5187	2.4	
Pb	2	0.01	0.40	<0.40	2.01	3.88	5.79	8.27	10.6	14.1	18.4	22.6	28.5	367	3.3	
Pd	912	0.010	0.010	<0.010	<0.010	<0.010	<0.010	<0.010	<0.010	<0.010	<0.010	<0.010	<0.010	0.013	0.052	1.0
Pt	946	0.002	0.004	<0.004	<0.004	<0.004	<0.004	<0.004	<0.004	<0.004	<0.004	<0.004	<0.004	<0.004	0.007	0.5
Rb	7	0.1	0.5	<0.5	1.4	2.6	3.7	5.7	8.5	13	20	25	32	68	2.4	
Re	954	0.001	0.010	<0.010	<0.010	<0.010	<0.010	<0.010	<0.010	<0.010	<0.010	<0.010	<0.010	<0.010	<0.010	<0.010
S	19	200	20	<20	22	33	48	74	116	187	284	380	575	4353	2.6	
Sb	37	0.020	0.020	<0.020	<0.020	0.024	0.030	0.044	0.067	0.105	0.173	0.257	0.454	13.0	3.1	
Sc	2	0.1	0.1	<0.1	0.4	0.7	1.1	2	2.4	3.1	3.9	4.8	6.2	17	2.5	
Se	736	0.1	0.5	<0.5	<0.5	<0.5	<0.5	<0.5	<0.5	<0.5	0.7	0.9	1.1	6.0	1.4	
Sn	81	0.10	0.10	<0.10	<0.10	<0.10	0.11	0.16	0.24	0.35	0.54	0.75	1.1	6.9	2.1	
Sr	2	0.5	0.5	<0.5	1.3	2.2	3.3	5.4	8.3	11	17	23	31	252	3.0	
Ta	954	0.05	0.05	<0.05	<0.05	<0.05	<0.05	<0.05	<0.05	<0.05	<0.05	<0.05	<0.05	<0.05	<0.05	
Te	834	0.02	0.07	<0.07	<0.07	<0.07	<0.07	<0.07	<0.07	<0.07	0.078	0.097	0.14	0.49	1.1	
Th	2	0.1	0.1	<0.1	0.4	0.9	1.6	3	4.3	6.1	7.9	9.8	12	15	2.5	
Ti	1	10	10	<10	52	157	276	485	755	1087	1607	2022	2587	7213	3.2	
Tl	48	0.02	0.02	<0.02	<0.02	<0.02	0.04	0.06	0.09	0.13	0.19	0.22	0.28	0.4	1.6	
U	4	0.1	0.1	<0.10	0.13	0.25	0.36	0.55	0.82	1.1	1.9	2.7	4.3	20	2.9	
V	9	2	2	<2.0	4.7	10	14	22	29	38	53	70	100	281	2.4	
W	629	0.05	0.05	<0.05	<0.05	<0.05	<0.05	<0.05	<0.05	0.06	0.12	0.17	0.25	2.0	1.9	
Y	0	0.01	0.01	0.21	1.0	1.7	2.2	3.9	5.8	8.1	12	16	22	92	2.6	
Zn	0	0.10	0.10	0.62	3.51	13.4	20.7	32.7	45.9	58.1	72.3	83.6	110	1335	3.3	
Zr	4	0.1	0.05	<0.05	0.28	0.58	0.94	1.8	2.8	4.1	5.8	7.2	9.1	23	3.0	

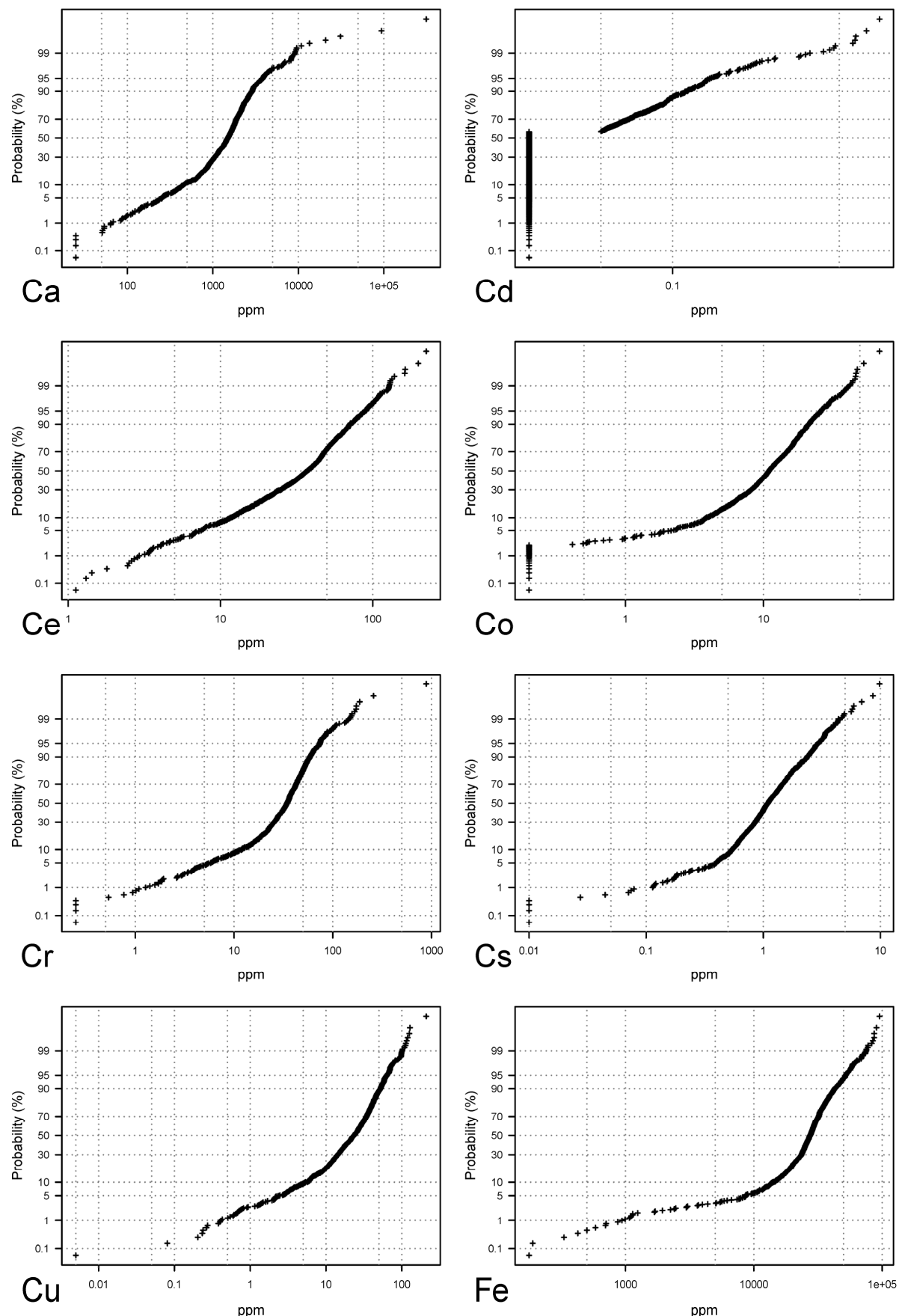
Table 5: Comparable geochemical statistics for three MINN surveys. Units in mg/kg.

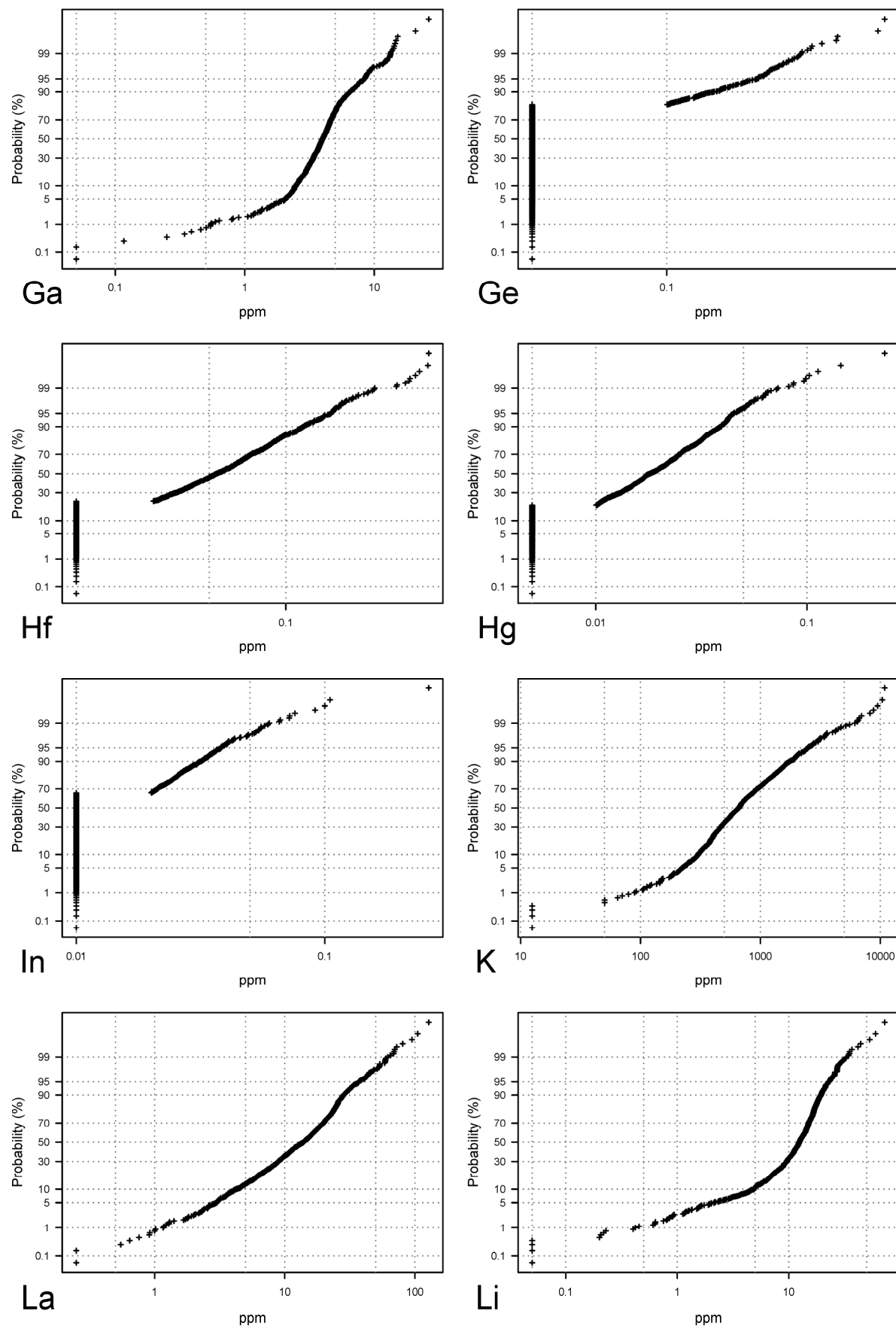
MINN 2013 - Hattfjelldal				MINN 2012 - Nord-Salten			MINN 2011 - Nordkinn			
Element	PDL	Q50	Q98	Max	Median	Q98	MAX	Median	Q98	MAX
Ag	0.005	0.025	0.194	0.65	0.012	0.10	3.1	0.011	0.077	0.22
Al	50	13935	29423	38640	7010	32600	86100	15105	25453	32809
As	1	7.52	47	498	1	7.8	81	2.3	18	67
Au	0.002	<0.002	0.008	0.054	0.0003	0.004	0.035	0.001	0.005	0.034
B	7	<7.0	<7.0	7.3	<1	1.8	14	<1	2.2	3.8
Ba	0.5	17	78	262	18	213	596	45	127	190
Be	0.1	0.23	0.76	1.7	0.2	0.8	2.4	0.3	0.9	1.9
Bi	0.02	0.13	0.35	2.2	0.09	0.39	3.3	0.1	0.4	1.0
Ca	50	1504	6689	313558	720	6460	274000	619	2357	11714
Cd	0.05	<0.05	0.22	0.74	0.02	0.13	0.66	0.02	0.13	0.71
Ce	0.1	37.1	110	225	38	190	593	54	174	799
Co	0.4	11	35	69	2.4	23	65	10	20	179
Cr	0.5	34	101	885	7.7	104	343	21	43	187
Cs	0.02	1.1	3.8	9.8	1.1	5.6	9.8	2.8	5.9	11
Cu	0.01	23.4	81.3	210	4.3	66	390	16	42	660
Fe	100	27476	62888	95312	17300	46400	70300	28010	45063	158298
Ga	0.1	4.00	11.6	26.4	5.4	15	27	5	9	12
Ge	0.1	<0.10	0.18	0.31	<0.1	0.30	0.43	<0.1	0.23	0.46
Hf	0.030	0.053	0.18	0.37	0.03	0.13	0.39	0.09	0.25	0.57
Hg	0.010	0.018	0.059	0.23	0.011	0.052	0.180	0.011	0.04	0.17
In	0.020	<0.020	0.052	0.26	0.02	0.09	0.23	<0.02	0.04	0.07
K	25	663	3596	10871	1210	10700	18900	3712	8298	12902
La	0.5	14	53	128	18	91	438	20	82	408
Li	0.10	12	27	73	7.9	46	83	12	29	59
Mg	100	7204	19812	85382	2090	21500	60800	4933	9280	21057
Mn	10	335	1344	5042	129	812	2410	229	791	18372
Mo	0.01	0.54	3.6	18	0.91	28	136	4	23	
Na	5.0	32	142	626	56	376	2530	38	122	373
Nb	0.05	0.72	3.7	16	2.4	11	18	1.6	4.1	6.5
Ni	0.3	25	80	364	3.5	60	133	18	32	81
P	10	516	1481	5187	285	1580	2970	357	890	2126
Pb	0.40	10.6	28.5	367	6.6	26	454	8.9	28	134
Pd	0.010	<0.010	0.013	0.052	<0.01	<0.01	0.030	<0.01	0.011	0.023
Pt	0.004	<0.004	<0.004	0.007	<0.002	<0.002	0.009	<0.002	0.002	0.004
Rb	0.5	8.5	32	68	20	90	195	42	83	135
Re	0.010	<0.010	<0.010	<0.010	<0.001	0.001	0.002	<0.001	0.002	0.003
S	20	116	575	4353	126	733	4520	110	440	1746
Sb	0.020	0.067	0.454	13.0	0.04	0.21	1.7	0.11	0.38	1.2
Sc	0.1	2.4	6.2	17	1.9	9.0	21	1.9	3.6	5.7
Se	0.5	<0.5	1.1	6.0	0.2	1.8	6.0	0.4	1.2	4.1
Sn	0.10	0.24	1.1	6.9	0.9	3.2	81	0.6	1.1	1.7
Sr	0.5	8.3	31	252	2.5	25	1260	5.6	23	52
Ta	0.05	<0.05	<0.05	<0.05	<0.05	<0.05	0.09	<0.05	<0.05	<0.05
Te	0.07	<0.07	0.14	0.49	<0.02	0.10	0.34	<0.02	0.05	0.08
Th	0.1	4.3	12	15	5.1	28	51	5	11	20
Ti	10	755	2587	7213	1280	3710	5540	1527	3060	4303
Tl	0.02	0.09	0.28	0.4	0.16	0.69	1.5	0.30	0.60	1.9
U	0.1	0.82	4.3	20	1.2	18	120	1.0	4	34
V	2	29	100	281	19	105	191	29	56	89
W	0.05	<0.05	0.25	2.0	0.1	0.8	2.3	<0.1	<0.1	0.2
Y	0.01	5.8	22	92	6.4	29	81	10	42	163
Zn	0.10	45.9	110	1335	28	113	317	49	94	254
Zr	0.05	2.8	9.1	23	0.9	5	16	4	12	29

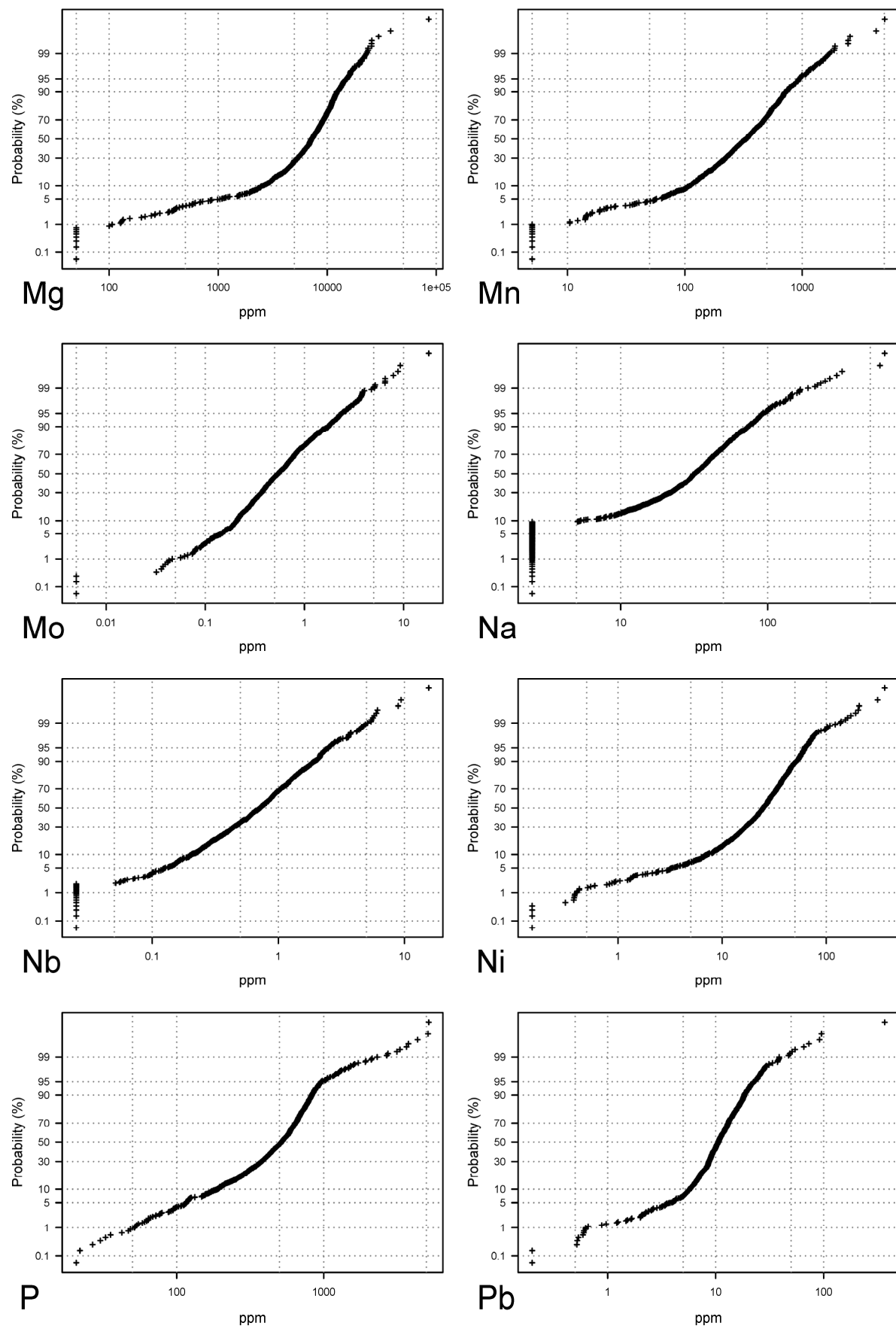
Appendix 1: Cumulative frequency diagrams

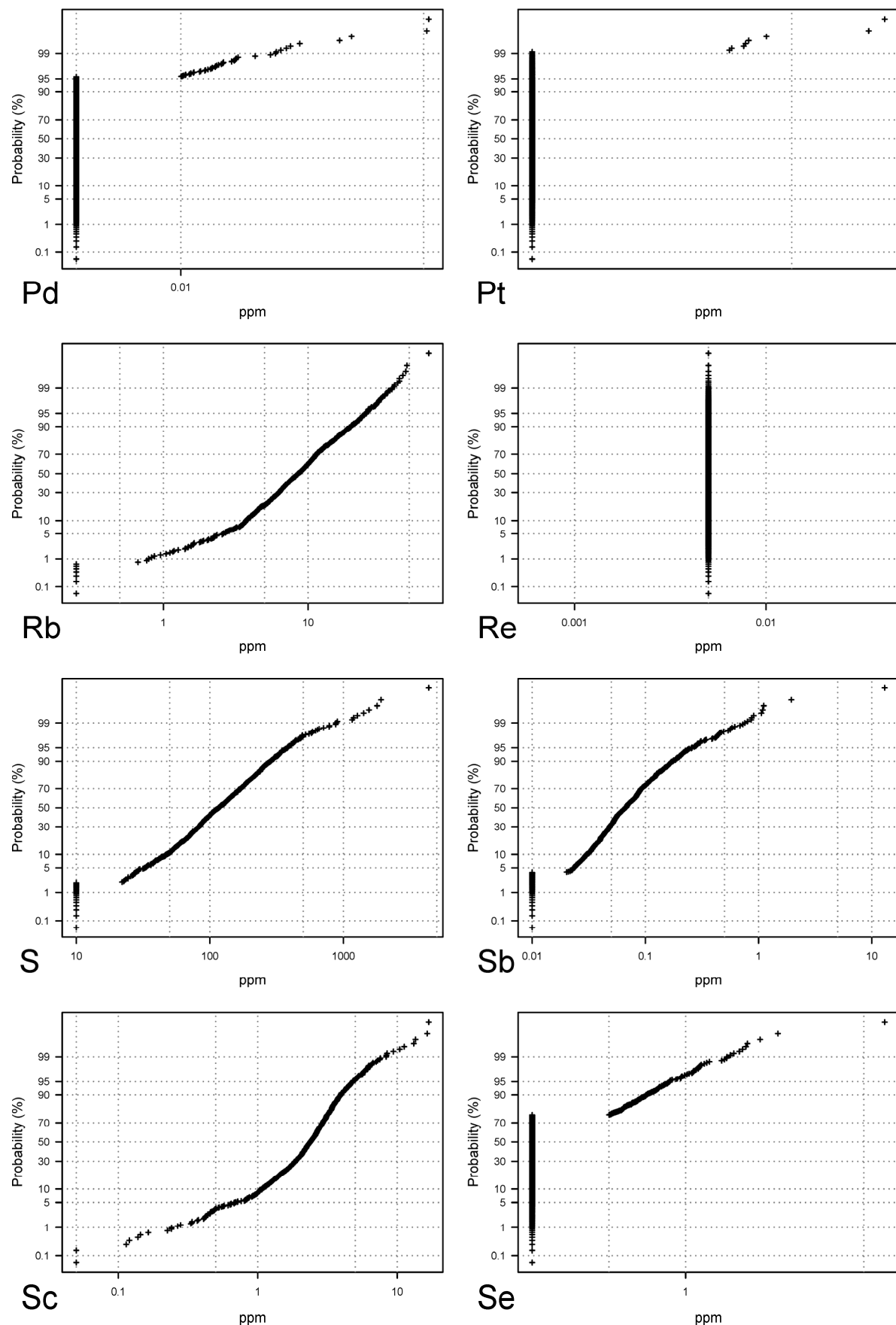
Please note that readings below the practical detection limit are set to half of the practical detection limit value.

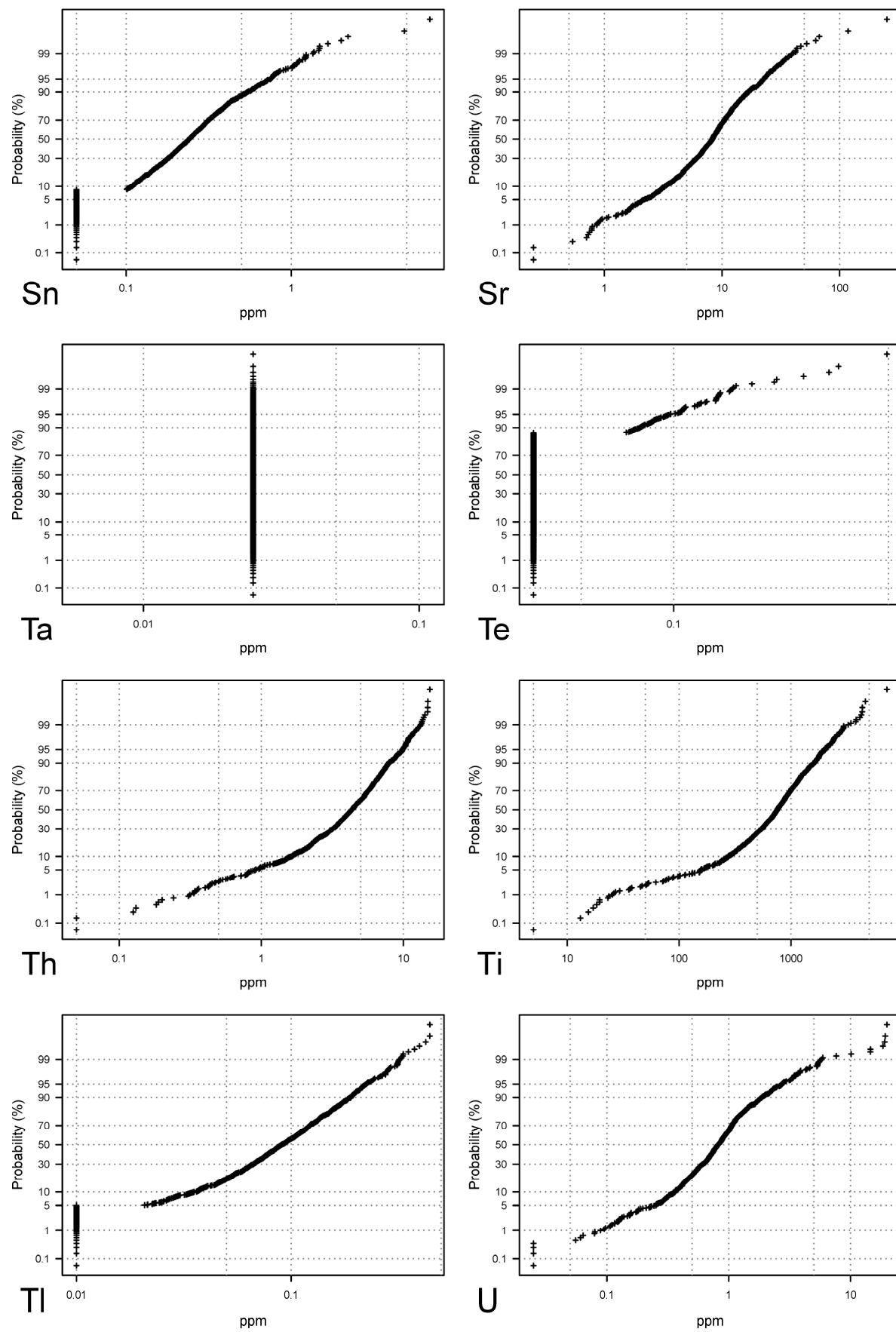


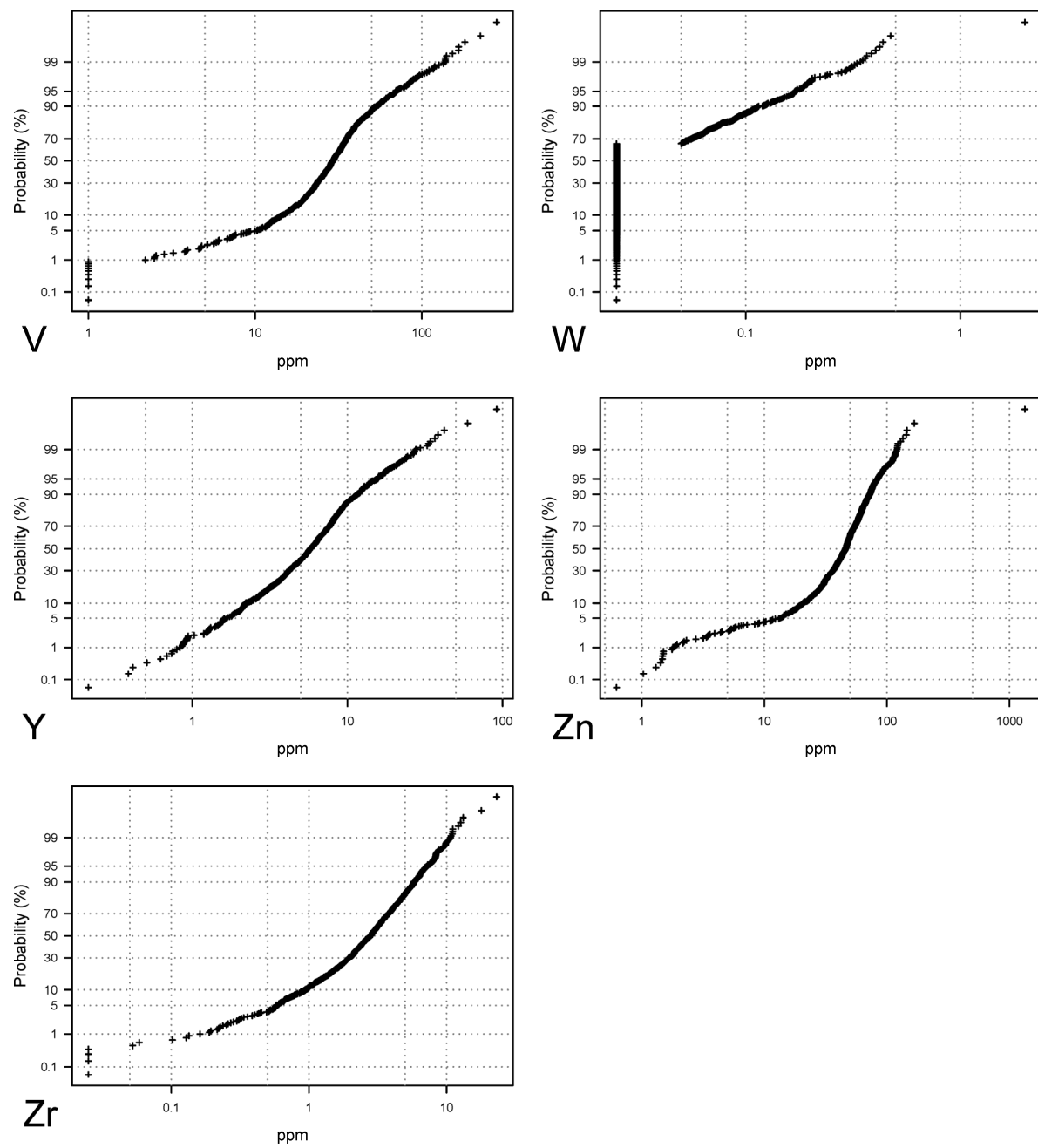












Appendix 2: Geochemical maps from the Hattfjelldal area

